Approximate expression for the electric potential around an absorbing particle in isotropic collisionless plasma

I. L. Semenov, S. A. Khrapak, and H. M. Thomas

Citation: Physics of Plasmas (1994-present) **22**, 053704 (2015); doi: 10.1063/1.4921249
View online: http://dx.doi.org/10.1063/1.4921249
View Table of Contents: http://scitation.aip.org/content/aip/journal/pop/22/5?ver=pdfcov
Published by the AIP Publishing

Approximate expression for the electric potential around an absorbing particle in isotropic collisionless plasma

I. L. Semenov,[1,a)] S. A. Khrapak,[1,2,b)] and H. M. Thomas[1]
[1]*Forschungsgruppe Komplexe Plasmen, Deutsches Zentrum für Luft- und Raumfahrt, Oberpfaffenhofen, Germany*
[2]*Aix-Marseille-Université, CNRS, Laboratoire PIIM, UMR 7345, 13397 Marseille cedex 20, France*

(Received 17 March 2015; accepted 6 May 2015; published online 15 May 2015)

A new approximate expression for the potential distribution around an absorbing particle in isotropic collisionless plasma is proposed. The approximate expression is given by the sum of the Debye-Hückel potential with an effective screening length and the far-field asymptote obtained from the solution of the linearized Poisson equation. In contrast to analogous models, the effective screening length is not fixed but depends on the distance from the particle. This allows us to obtain a more accurate approximation for the potential distribution in the entire range of distances. The dependence of the screening length on the distance is predicted from the analysis of the charge density distribution function. This dependence contains two adjustable parameters, which are calculated by applying the procedure based on charge balance considerations. Using the obtained results, simple expressions for the parameters of the model are proposed. In addition, a simple expression for the characteristic screening length, which can be used to approximate the potential distribution near the particle, is obtained. The developed model potential is shown to be in excellent agreement with the solution of the nonlinear Poisson equation for typical conditions used in experiments with complex plasmas. © *2015 AIP Publishing LLC*.
[http://dx.doi.org/10.1063/1.4921249]

I. INTRODUCTION

Screening of a charged particle immersed in plasma is one of the classical problems in plasma physics. It has received renewed attention recently in view of its significance for understanding properties of complex (dusty) plasma—weakly ionized gas containing micron-sized particles as an additional component.[1–4] During the last decades, complex plasma has been recognized as a suitable model for studying basic phenomena in strongly coupled systems.[5–7] This feature of complex plasmas has given rise to extensive theoretical studies and experimental research including both ground-based and microgravity experiments.[8–10] Other aspects of complex plasma physics include also technological applications,[11] astrophysical problems[12] and fusion related problems.[13,14]

Under typical conditions, particles in complex plasmas acquire a high negative charge due to absorption of ions and electrons. In this case, plasma near the particle is far from thermodynamic equilibrium and, therefore, the screening process has to be described within the framework of the kinetic theory rather than using the conventional Poisson-Boltzmann approach. The problem is simplified when surrounding plasma is assumed to be isotropic and collisionless. The first assumption can be justified when the particles levitate in the bulk of the plasma discharge (e.g., for complex plasmas under microgravity conditions). The second assumption is more restrictive, since it is justified only when the gas pressure is sufficiently low. However, it is often accepted as a reasonable simplification in many studies.

For the case of isotropic collisionless plasma, the exact potential distribution can be obtained by solving the nonlinear Poisson equation with the charge density derived from the solution of the stationary Vlasov equation.[15,16] Since the nonlinear Poisson equation can be solved only numerically, approximate expressions are usually applied to predict the potential distribution with certain accuracy. The common approach in this case is to use an analytical solution of the linearized Poisson equation. The corresponding solution is given by the sum of the Debye-Hückel (DH) potential with the linearized Debye length λ_D and the far-field asymptote which is approximately proportional to r^{-2}, where r is the distance from the particle center. The linearization is valid, however, only for small values of the nonlinearity parameter[17] $\beta = (a/\lambda_{Di})(|\varphi_a|/kT_e)(T_e/T_i)$, where a is the particle size, λ_{Di} is the ion Debye length, φ_a is the particle potential, and $T_{i,e}$ are the temperatures of ions and electrons in plasma, respectively. Note that in typical complex plasmas $\lambda_{Di} \approx \lambda_D$, since $T_e \gg T_i$.

The linear theory becomes inapplicable at high values of the nonlinearity parameter ($\beta \sim 10$–100) due to strong ion-particle coupling. As it was shown in Refs. 18 and 19, for this regime, the exact solution near the particle ($r \lesssim \lambda_{Di}$) is still well approximated by the DH potential if some effective screening length $\lambda_s > \lambda_D$ is used. In Ref. 19, the effective screening length λ_s was also found to depend only on the parameter β. Simple approximations to the function $\lambda_s(\beta)$ were proposed in Refs. 19 and 20. It can be demonstrated, however (see Sec. II), that at intermediate distances ($r \lesssim 10\lambda_{Di}$)

a)Electronic mail: Igor.Semenov@dlr.de
b)Also at Joint Institute for High Temperatures, Russian Academy of Sciences, Moscow, Russia.

the DH potential with the constant effective screening length λ_s gives a poor approximation to the exact solution. Behavior of the potential in this range might have an influence on formation and properties of three dimensional particles structures usually studied in microgravity experiments with complex plasmas. Therefore, it would be desirable to find a more accurate approximation for the potential distribution in the entire range of distances.

In the present work, a new approximate expression for the electric potential distribution around an absorbing particle in isotropic collisionless plasma is proposed. The underlying idea is based on the assumption that the effective screening length in the DH potential is not fixed but depends on the distance from the particle. The functional form of this dependence is predicted from the analysis of the nonlinear charge density distribution. The obtained model potential contains two adjustable parameters which are calculated by applying the procedure based on charge balance considerations. The adjustable parameters are shown to depend only on the nonlinearity parameter β, and simple approximations to the corresponding functions are suggested. It is shown that the developed model potential is in excellent agreement with the results obtained from the numerical solution of the nonlinear Poisson equation up to $\beta \sim 100$. On the basis of the proposed model, we also find an expression for the characteristic screening length which can be used to approximate the potential distribution near the particle.

The structure of the paper is as follows. In Sec. II, the screening theory based on the nonlinear Poisson equation is used to find the exact potential distribution for typical laboratory conditions. In addition, the comparison of the exact solution with the existing model potentials is shown. In Sec. III, a new approximate expression for the potential distribution is derived and the comparison with the exact solution is presented. The range of applicability of the proposed model is discussed. Conclusions are summarized in Sec. IV.

II. NONLINEAR SCREENING THEORY

As it was mentioned in the Introduction, the exact potential distribution around an absorbing particle in isotropic collisionless plasma can be obtained using the nonlinear Poisson equation with the charge density derived from the solution of the Vlasov equation. The corresponding Poisson equation was first presented in Ref. 15 and explained in more details in Ref. 16. For clarity, we repeat this equation in the present work.

Let us consider a spherical particle of radius a immersed in isotropic plasma consisting of singly ionized ions, electrons, and neutral atoms. The influence of collisions between plasma components on the charging and screening processes is neglected. Far from the particle, the velocity distribution functions of ions and electrons are assumed to be Maxwellian with the number density n_0 and temperatures T_i and T_e, respectively. It is also assumed that the particle is charged due to surface absorption of ions and electrons. Under these conditions, the normalized particle potential $\alpha_\mathrm{e} = -e\varphi_a/kT_\mathrm{e}$ is usually of the order of unity and can be well estimated using the orbital motion limited (OML) theory.[3,21]

For isotropic plasma, the potential distribution around the particle can be found by solving the Poisson equation

$$\Delta\varphi = -4\pi e[n_\mathrm{i}(r,\varphi) - n_\mathrm{e}(r,\varphi)], \tag{1}$$

where $\Delta = r^{-2}\,\partial/\partial r(r^2\,\partial/\partial r)$, e is the elementary charge, φ is the electric potential, and $n_{\mathrm{i,e}}$ are the ion and electron number densities, respectively. To proceed further, we introduce the following dimensionless variables:

$$x = r/a, \quad \tau_\mathrm{e} = T_\mathrm{e}/T_\mathrm{i}, \quad \varphi_\mathrm{e} = -e\,\varphi/kT_\mathrm{e}, \quad \varphi_\mathrm{i} = \varphi_\mathrm{e}\tau_\mathrm{e}.$$

Then, the ion number density can be written as a sum

$$n_\mathrm{i} = n_1 + n_2, \tag{2a}$$

where[15,16]

$$\frac{n_1}{n_0} = \sqrt{\frac{\varphi_\mathrm{i}}{\pi}} + \frac{1}{2}\,\mathrm{erfcx}\left(\sqrt{\varphi_\mathrm{i}}\right), \tag{2b}$$

and

$$\frac{n_2}{n_0} = \sqrt{\frac{f_\mathrm{i}}{\pi}} + \frac{1}{2}\,\mathrm{erfcx}\left(\sqrt{f_\mathrm{i}/g}\right)\sqrt{g}, \ \text{for } f_\mathrm{i} \geq 0, \tag{2c}$$

$$\frac{n_2}{n_0} = \frac{1}{2}\,\exp(\varphi_\mathrm{i})\sqrt{g}, \ \text{for } f_\mathrm{i} < 0. \tag{2d}$$

Here

$$g = 1 - x^{-2}, \quad f_\mathrm{i} = \varphi_\mathrm{i} - \alpha_\mathrm{e}\,\tau_\mathrm{e}\,x^{-2},$$

and $\mathrm{erfcx}(\xi) = \exp(\xi^2)\,[1 - \mathrm{erf}(\xi)]$ is the scaled complementary error function. The electron number density is given by[15,16,21]

$$n_\mathrm{e}/n_0 = (1/2)\,\exp(-\varphi_\mathrm{e})[\,1 + \mathrm{erf}(\sqrt{f_\mathrm{e}}) + \exp\,(f_\mathrm{e}/gx^2)\mathrm{erfc}(\sqrt{f_\mathrm{e}/g})\sqrt{g}\,], \tag{3}$$

where $f_\mathrm{e} = \alpha_\mathrm{e} - \varphi_\mathrm{e}$.

At large distances from the particle, where $\varphi_{\mathrm{i,e}} \ll 1$, Eqs. (2a) and (3) can be linearized. The corresponding Poisson equation is written as

$$\Delta\varphi_\mathrm{e} = k_0^2\,(\,\varphi_\mathrm{e} - \omega_0/x^2\,), \tag{4}$$

where

$$\omega_0 = (1 + 2\alpha_\mathrm{e}\tau_\mathrm{e})/4(1 + \tau_\mathrm{e}),$$

$k_0 = \lambda_\mathrm{D}^{-1}$ and λ_D is the linearized Debye length given by

$$\lambda_\mathrm{D} = \lambda_\mathrm{Di}\sqrt{\tau_\mathrm{e}/(1 + \tau_\mathrm{e})}.$$

Here, $\lambda_\mathrm{Di} = (4\pi e^2 n_0/kT_\mathrm{i})^{-1/2}$ is the ion Debye length.

Equation (4), along with the conditions

$$\varphi_\mathrm{e} = \alpha_\mathrm{e} \text{ at } r = a, \quad \varphi_\mathrm{e} \to 0 \text{ as } r \to \infty, \tag{5}$$

has an analytical solution, which can be written as

$$\varphi_e(r) = \frac{\hat{\alpha}_e}{x}\exp(-k_0 y) + \psi_e(r), \tag{6a}$$

where $y = r - a$, $\hat{\alpha}_e = \alpha_e - \psi_{e,r=a}$ and

$$\psi_e(r) = \omega_0 (a k_0)^2 \mathcal{F}(r k_0). \tag{6b}$$

Here, $\mathcal{F}(\xi) = [e^{-\xi}\,\mathrm{Ei}(\xi) - e^{\xi}\,\mathrm{Ei}(-\xi)]/2\xi$, where $\mathrm{Ei}(\xi)$ is the exponential integral. One can see that the solution of the linearized Poisson equation is given by the sum of the DH potential with the linearized Debye length λ_D and the far-field asymptote ψ_e. Note that, since $\mathcal{F}(\xi) \approx \xi^{-2}$ at $\xi \to \infty$, the potential ψ_e far from the particle tends to the power-law asymptote known from the probe theory.[3]

The solution of the nonlinear Poisson equation (1) with the conditions (5) can be obtained only numerically. To find this solution, we consider Eq. (1) on the finite interval $a \le r \le r_m$ with the following boundary conditions

$$\varphi_e = \alpha_e \quad \text{at} \quad r = a, \quad \varphi_e = \psi_e \quad \text{at} \quad r = r_m, \tag{7}$$

where r_m is chosen to be sufficiently large ($r_m \gtrsim 20\lambda_{Di}$). Note that far from the particle, the exact solution tends to the asymptote ψ_e, thus, the condition $\varphi_e = \psi_e$ seems to be a reasonable choice at $r_m \gg \lambda_{Di}$. The corresponding boundary-value problem is solved by means of the conventional shooting method. Namely, we first solve the Cauchy problem for Eq. (1) with the initial conditions $\varphi_e = \alpha_e$, $\partial\varphi_e/\partial r = -qe/kT_e a^2$, where q is the absolute value of the particle charge. Then, the value of q is adjusted to satisfy the condition $\varphi_e = \psi_e$ at $r = r_m$. The Cauchy problem for Eq. (1) is solved numerically by means of the fourth-order explicit Runge-Kutta method.

The numerical results were obtained for typical experimental conditions. Namely, τ_e was varied from 10 to 250, and the particle size was varied in the range $a \lesssim 0.1\lambda_{Di}$. The particle potential was calculated via the OML flux balance equation[3,21] assuming that the particle is immersed in neon plasma (note, that neon is used in the forthcoming microgravity experiment PK-4 (Ref. 10)).

The potential distributions obtained from the solution of the nonlinear Poisson equation (1) are presented in Fig. 1 for different values of the nonlinearity parameter $\beta = (a/\lambda_{Di})\alpha_e\tau_e$. In addition, we also show in Fig. 1 the solution of the linearized Poisson equation (see Eq. (6a)) and the model potential obtained using the results presented in Refs. 18 and 19. This potential reads as

$$\varphi_e(r) = \frac{\hat{\alpha}_e}{x}\exp(-k_s y) + \psi_e(r), \tag{8}$$

where $k_s = \lambda_s^{-1}$ and λ_s is the effective screening length. In Refs. 18 and 19, the effective screening length was chosen in such a way that the DH part of the potential (8) gives the best possible approximation to the exact solution in the range $r \lesssim \lambda_D$. It was also found in Ref. 19 that the effective screening length λ_s depends only on the parameter β. The corresponding dependence proposed in Ref. 19 is given by

$$\lambda_s/\lambda_{Di} = 1 + 0.2\sqrt{\beta}, \tag{9}$$

where $\beta \lesssim 10$. Another approximation to the function $\lambda_s(\beta)$ was proposed in Ref. 20 using the results of Ref. 18. This approximation reads as

$$\lambda_s/\lambda_{Di} = 1 + 0.013\,\beta + 0.105\sqrt{\beta}, \tag{10}$$

where $\beta \lesssim 100$. It is worth noting that the results of Ref. 18 were obtained using a simplified model which assumes that the distribution function of ions in undisturbed plasma is monoenergetic. Thus, for moderate values of β it is more reliable to use Eq. (9). From the other hand, Eq. (10) can be used to estimate the screening length at high values of β.

One can observe from Fig. 1 that in the nearly linear regime (Fig. 1(a)) both the solution given by Eq. (6a) and the model potential given by Eq. (8) provide a reasonable approximation to the exact solution. However, as the nonlinearity parameter increases (Figs. 1(b)–1(d)), the approximations given by Eqs. (6a) and (8) become less accurate. The deviations from the exact solution are especially noticeable in the intermediate range of distances ($r \lesssim 10\lambda_{Di}$). As it was mentioned before, behavior of the potential in this range can influence the properties of large three dimensional particles structures studied in microgravity experiments with complex plasmas. It would be desirable, therefore, to find a more accurate approximation for the potential distribution in the nonlinear regime.

III. NEW MODEL POTENTIAL

In this section, we present a new approximate expression for the electric potential distribution around an absorbing particle in isotropic collisionless plasma. In order to clarify the underlying idea, we start with some preliminary considerations.

A. Preliminary considerations

First, one can show that the solution of the nonlinear Poisson equation (1) with the conditions (5) is rather well approximated by the potential

$$\varphi_e(r) = \varphi_e^*(r) + \psi_e(r), \tag{11}$$

where φ_e^* is the solution of the nonlinear Poisson equation with the conditions

$$\varphi_e = \hat{\alpha}_e \quad \text{at} \quad r = a, \ \varphi_e \to 0 \quad \text{as} \quad r \to \infty, \tag{12}$$

and the charge density $en_0\rho(\varphi_i)$, where

$$\rho(\varphi_i) = 2\sqrt{\frac{\varphi_i}{\pi}} + \mathrm{erfcx}\left(\sqrt{\varphi_i}\right) - \exp(-\varphi_i/\tau_e). \tag{13}$$

The function given by Eq. (13) can be obtained from the following considerations. It is known that the main effect on the screening process comes from the region near the maximum of the function $(n_i - n_e)r^2$ which usually occurs at $r \sim 1 - 3\lambda_{Di}$. Most of the space charge which screens the particle resides in this region, where the following relations are valid: $x \gg 1$, $g \approx 1$, and $\varphi_i \gg \alpha_e\tau_e x^{-2}$, i.e., $f_i \approx \varphi_i$. One can conclude from Eqs. (2b) and (2c) that in this case the ion

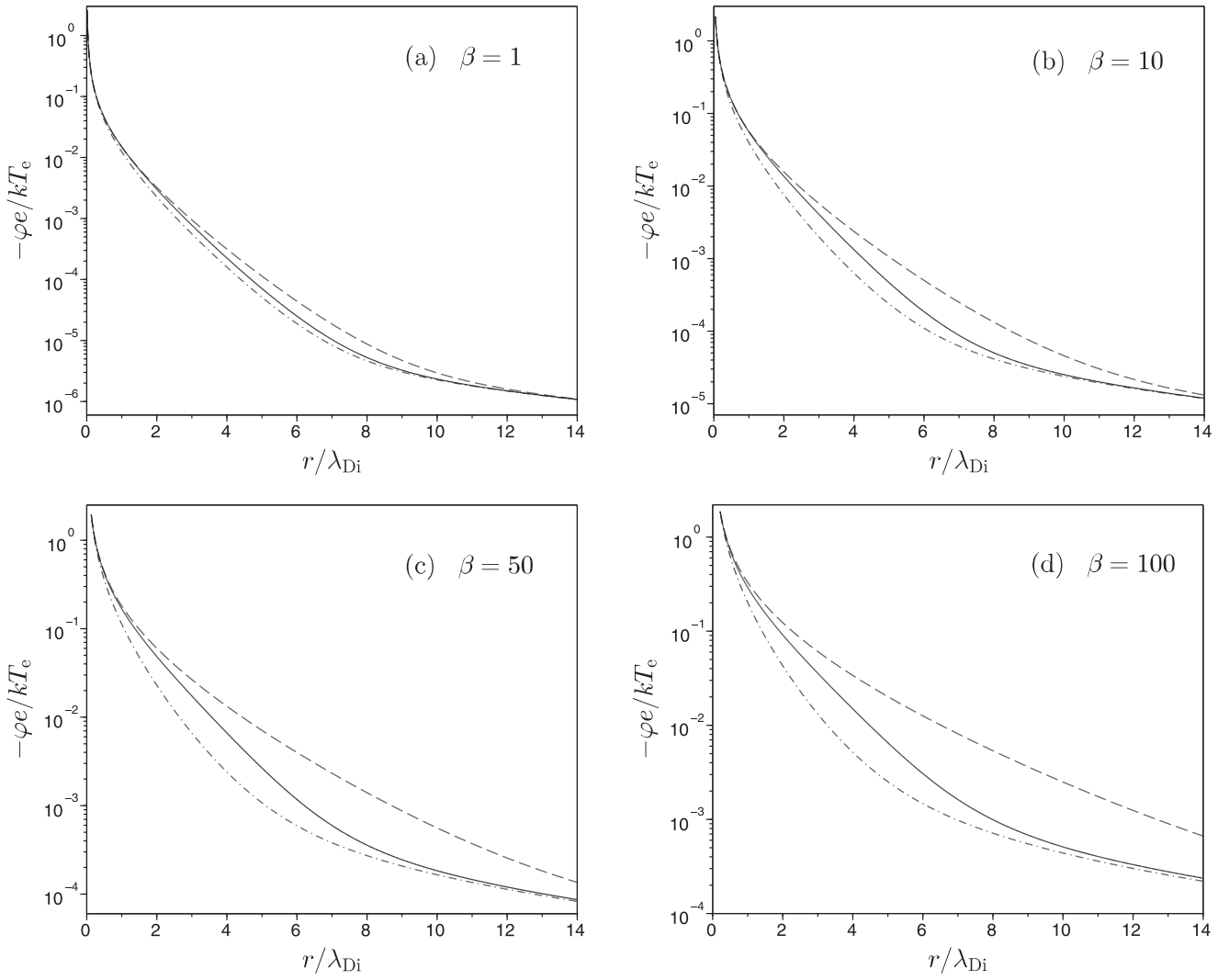

FIG. 1. The electric potential distribution around the particle for different values of the nonlinearity parameter: $\beta = 1$, $\tau_e = 30$, $a \approx 0.01\lambda_{Di}$ (a); $\beta = 10$, $\tau_e = 100$, $a \approx 0.05\lambda_{Di}$ (b); $\beta = 50$, $\tau_e = 200$, $a \approx 0.1\lambda_{Di}$ (c); $\beta = 100$, $\tau_e = 250$, $a \approx 0.2\lambda_{Di}$ (d). The solid line shows the numerical solution of the nonlinear Poisson equation (1), the dashed line shows the model potential given by Eq. (8) and the dashed-dotted line shows the solution of the linearized Poisson equation given by Eq. (6a). The screening length λ_s in Eq. (8) is given by Eq. (9) for the cases (a), (b) and by Eq. (10) for the cases (c), (d).

density can be approximately written as $n_i/n_0 = 2\sqrt{\varphi_i/\pi} + \mathrm{erfcx}(\sqrt{\varphi_i})$. The same function can also be obtained from the integration of the ion distribution function over the velocity space using the condition of positive ion energy.[22] The electron density distribution is usually well described by the conventional Boltzmann factor. The exact distribution (3) deviates from the Boltzmann law only near the particle surface. The above considerations lead directly to the function (13).

The nonlinear Poisson equation with the normalized charge density (13) and conditions (12) can be solved numerically using the same procedure as was used for solving Eq. (1). The only difference is the boundary condition at $r = r_m$. Note that the solution of the Poisson equation with the linearized form of the charge density (13) is given by the conventional DH potential (see the first term in Eq. (6a)). Thus, far from the particle at $r = r_m$, one can use the boundary condition $\partial\varphi/\partial r = -\varphi\,(k_0 + r_m^{-1})$.[23]

In Fig. 2, we show the comparison between the solution of Eq. (1) and the potential given by Eq. (11) for different values of β. One can see that the presented potentials are in excellent agreement. It means that if one finds an appropriate approximation φ_e^* to the solution of the Poisson equation with the charge density given by Eq. (13), then the approximation to the solution of the original nonlinear Poisson equation (1) can be simply given by the sum $\varphi_e = \varphi_e^* + \psi_e$. Therefore, we proceed further with the analysis of the function (13).

The right hand side of the Poisson equation with the normalized charge density (13) can be written as

$$-4\pi e n_0\, \rho(\varphi_i) = k_\rho^2\, \varphi,$$

where

$$k_\rho(\varphi_i(r)) = \lambda_{Di}^{-1}\, \sqrt{\rho(\varphi_i(r))/\varphi_i(r)}. \tag{14}$$

The expression $k_\rho^2\,\varphi$ is similar to the first term in the right hand side of the linearized Poisson equation given by Eq. (4). In this case, k_ρ^{-1} can be considered as an effective screening length which is not constant but depends on the distance from the particle. One can demonstrate that if the potential φ_i has a DH form with some screening length λ_s, the dependence $k_\rho(r)$ can be rather well approximated by the function

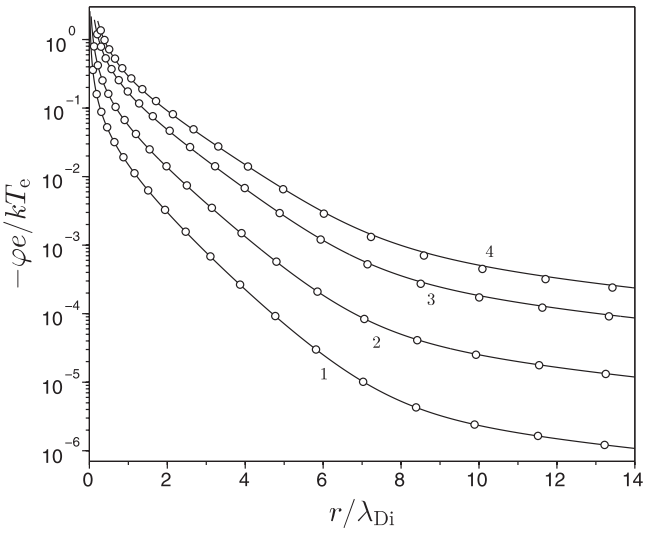

FIG. 2. Comparison between the potential given by Eq. (11) (circles) and the numerical solution of the nonlinear Poisson equation (1) (solid line). The potential distributions are shown for different values of the nonlinearity parameter: $\beta = 1$ (1), $\beta = 10$ (2), $\beta = 50$ (3), $\beta = 100$ (4). The corresponding values of τ_e and a are the same as in Fig. 1.

$$k_\rho \approx k_* + (k_0 - k_*)\tanh(c_* y), \tag{15}$$

where k_* and c_* are positive adjustable parameters. This approximation works well at least for high and moderate values of β. As an example, we show in Fig. 3(a) the comparison between the functions (14) and (15) for the case $\lambda_s = \lambda_D$ for two different values of β. The parameters k_* and c_* have been chosen to obtain the best possible fit to the function (14). The corresponding values of these parameters are given in the caption of Fig. 3. One can see from Fig. 3(a) that at high values of β, the functions (14) and (15) coincide in the entire range of distances. At lower values of β, the approximation (15) does not work so well in the vicinity of the particle, but it still provides a good approximation in the main region of interest, i.e., near the maximum of the charge distribution function. In order to illustrate this, we show in Fig. 3(b) the function $w_\rho = (k_\rho r)^2 \varphi_i$ for $\beta = 10$ with k_ρ given by Eq. (14) and Eq. (15). One can see from Fig. 3(b) that the approximation (15) indeed works well in the region near the maximum of the function w_ρ. It is worth noting, in addition, that for other values of λ_s the function (15) also provides a good approximation to the dependence (14).

Taking into account the above remark, it can be surmised that the approximate expression for the solution of the Poisson equation with the charge density (13) and conditions (12) can be given by

$$\varphi_e^* = \frac{\hat{\alpha}_e}{x}\exp(-s(y)), \tag{16}$$

where $s(y)$ is a screening factor depending on the distance from the particle. Substituting the potential (16) into the Poisson equation with the charge density (13), we obtain the following residual

$$\delta(\varphi_e^*) = \Delta\varphi_e^* - (k_\rho(\varphi_i^*))^2 \varphi_e^*, \tag{17}$$

where $\varphi_i^* = \varphi_e^* \tau_e$ and

$$\Delta\varphi_e^* = \varphi_e^* [(\partial s/\partial y)^2 - \partial^2 s/\partial y^2].$$

Neglecting the term $\partial^2 s/\partial y^2$, we use the condition $\delta(\varphi_e^*) = 0$ to obtain the equation for $s(y)$:

$$\partial s/\partial y = k_\rho. \tag{18}$$

If k_ρ is approximated via the function (15), then Eq. (18) has the following solution:

$$s(y) = k_* y + (k_0 - k_*)\ln(\cosh(c_* y))/c_*. \tag{19}$$

Note that for $s(y)$ given by Eq. (19), we have

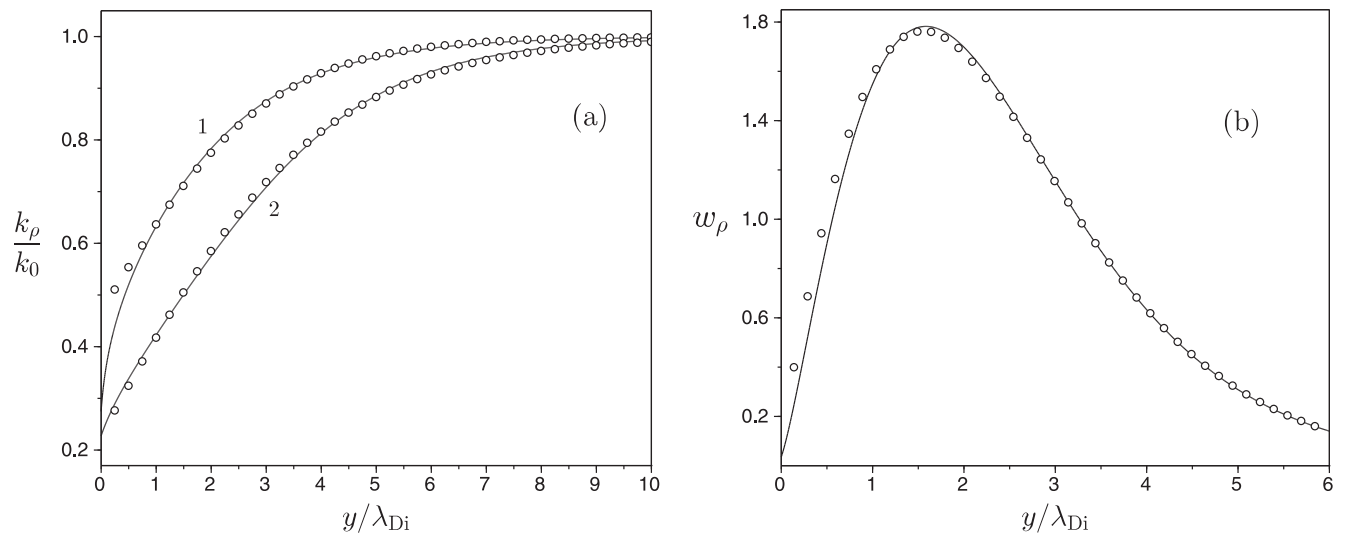

FIG. 3. The effective screening length (a) and charge distribution function (b) versus the distance from the particle. The effective screening length is presented for $\beta = 10$ (1) and $\beta = 100$ (2). The charge distribution function is presented for $\beta = 10$. The corresponding values of τ_e and a are the same as in Fig. 1. The solid lines show the results obtained using Eq. (14), where φ_i is the DH potential with the linearized Debye length λ_D. The circles show the results obtained using Eq. (15) with $k_* = 0.47\ k_0$, $c_* = 0.33\ k_0$ for $\beta = 10$, and $k_* = 0.23\ k_0$, $c_* = 0.25\ k_0$ for $\beta = 100$.

$$\partial^2 s/\partial y^2 = c_*(k_0 - k_*)(1 - \tanh(c_* y)^2).$$

It can be seen that the function $\partial^2 s/\partial y^2$ decreases rapidly with the distance and can be reasonably neglected in the residual (17) at least far from the particle. Therefore, the assumption made to derive the function (19) is justified. Using the function $s(y)$, one can easily define the effective screening length as $\lambda(y) = y/s(y)$. The corresponding inverse screening length $k(y) = \lambda(y)^{-1}$ is given by

$$k(y) = k_* + (k_0 - k_*)\ln(\cosh(c_* y))/(c_* y). \tag{20}$$

Note that $\ln(\cosh(\xi))/\xi \to 0$ as $\xi \to 0$, and, therefore, $k(y) \to k_*$ as $y \to 0$. In the opposite limit, we have $\ln(\cosh(\xi))/\xi \to 1$ as $\xi \to \infty$ and $k(y) \to k_0$ as $y \to \infty$.

In summary, we propose to use the potential (11) with φ_e^* given by Eq. (16) and the screening factor (19) as a new approximate expression for the solution of the Poisson equation (1) with the boundary conditions (5).

B. Parameters of the model

Let us further discuss the procedure to find the adjustable parameters k_* and c_*. From the physical point of view, it is convenient to consider these parameters in terms of their influence on the charge distribution functions

$$w = \Delta\varphi_i^* r^2, \quad w_\rho = (k_\rho(\varphi_i^*) r)^2 \varphi_i^*.$$

It is known that the charge distribution function usually has a maximum at $r \sim 1 - 3\lambda_{Di}$ (e.g., see Fig. 3(b)). The parameters k_* and c_* influence both the location and value of this maximum for the functions w and w_ρ. In particular, the parameter k_* mainly affects the relative distance between the maximum points. Let $r_m(c_*, k_*)$ and $r_{m,\rho}(c_*, k_*)$ denote the location of these points for the functions w and w_ρ, respectively. Then, for given c_*, the parameter k_* can be found using the following equation:

$$r_m(c_*, k_*) = r_{m,\rho}(c_*, k_*). \tag{21}$$

To be precise, one also has to define the interval where k_* must lie. The obvious choice for the upper bound of k_* is k_0. The lower bound k_a can be found using the condition $w = w_\rho$ at $r = a$. It leads to the quadratic equation

$$k_a^2 - c_*(k_0 - k_a) = (k_\rho(\hat{\alpha}_e \tau_e))^2. \tag{22}$$

One can see that this equation always has a real positive root. If Eq. (21) does not have a solution for $k_* \in [k_a, k_0]$, one can simply take $k_* = k_a$. Our calculations showed that the choice $k_* = k_a$ usually works well at high values of β. However, for small and moderate values of β, the better approximation is achieved when k_* is given by the solution of Eq. (21).

Using the function $k_*(c_*)$, one can find the parameter c_* from the condition

$$\int_a^\infty (w - w_\rho)\, dr = 0. \tag{23}$$

Equation (23) simply represents the fact that the total charge of the screening cloud is equal to the particle charge, which is defined by the derivative $\partial\varphi_i^*/\partial r$ at $r = a$. From the mathematical point of view, one can also say, that the parameter c_* is obtained using the weighted residual method. Namely, Eq. (23) means that the residual given by Eq. (17) is minimized in an integral sense with the weight r^2. Equations (21) and (23) defining the parameters k_* and c_* are the nonlinear equations, which can be solved numerically. In particular, the simplest choice is to solve these equations by means of the bisection method. The integral in Eq. (23) can also be evaluated numerically using, for example, the composite Simpson rule.

By employing the procedure described above, the parameters k_* and c_* were calculated for typical experimental conditions (see Sec. II). The obtained results show that the parameters k_* and c_* normalized to k_0 can be represented with good accuracy by the functions of the nonlinearity parameter β only. In fact, we present in Fig. 4 the dependence of the ratios k_*/k_0 and c_*/k_0 on the parameter β. One can see that the results obtained for different values of a and τ_e follow closely the same universal curves. Our computations showed that deviations from this universal behavior occur only at moderate values of τ_e, which are not frequent in complex plasma experiments. A possible fit to the results shown in Fig. 4 is given by

$$k_*/k_0 = (1 + 0.65\sqrt{\beta})^{-1/2}, \tag{24a}$$

$$c_*/k_0 = 1.72\,(1 + 1.2\sqrt{\beta})^{-1/2}. \tag{24b}$$

C. Results and discussions

Let us compare the proposed model potential with the solution of the nonlinear Poisson equation. In Fig. 5, we show the comparison between the solution of the equation (1) and the model potential (11), where φ_e^* is given by Eq. (16) with the screening factor (19) and the parameters k_* and c_* are

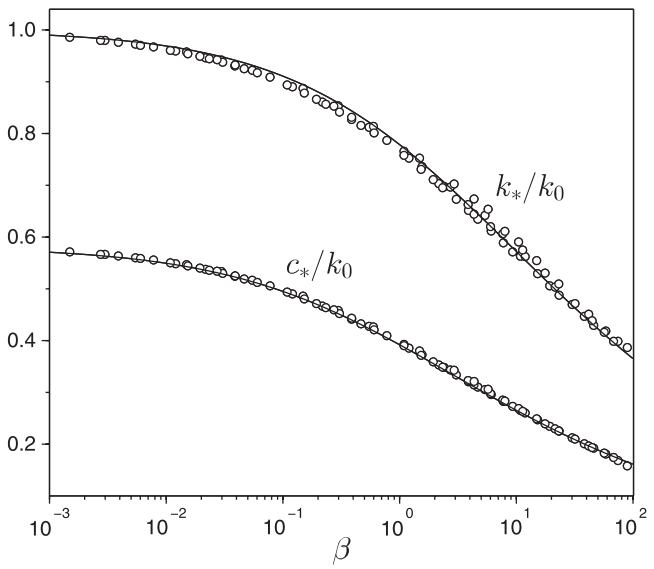

FIG. 4. The dependence of the ratios k_*/k_0 and c_*/k_0 on the nonlinearity parameter β. The circles show the results obtained for different values of a and τ_e using the procedure described in Sec. III B. The solid lines show the fit given by Eqs. (24a) and (24b).

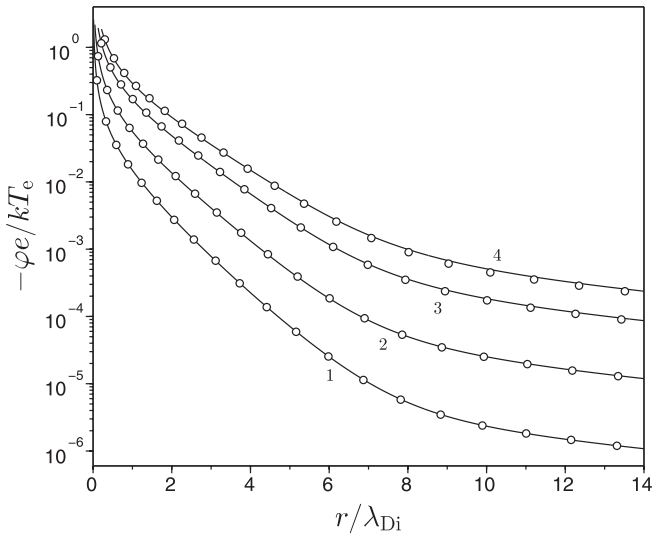

FIG. 5. Comparison between the model potential proposed in Sec. III A (circles) and the numerical solution of the nonlinear Poisson equation (1) (solid lines). The potential distributions are shown for different values of the nonlinearity parameter: $\beta = 1$ (1), $\beta = 10$ (2), $\beta = 50$ (3), $\beta = 100$ (4). The corresponding values of τ_e and a are the same as in Fig. 1.

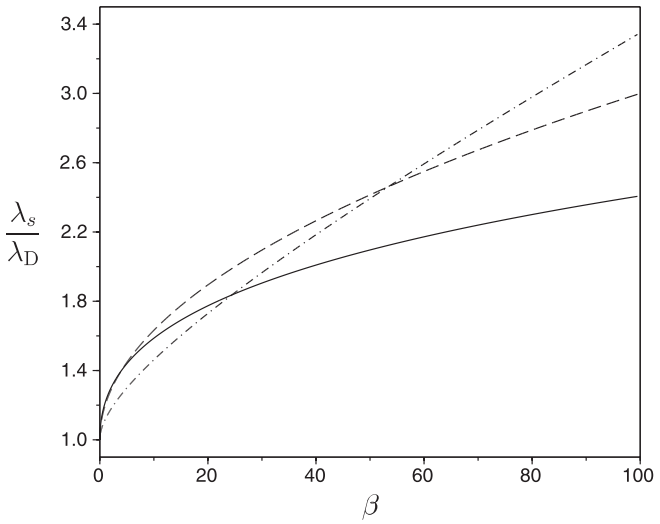

FIG. 6. The normalized effective screening length as a function of the nonlinearity parameter. The solid line shows the dependence given by Eq. (25), the dashed line shows the dependence given by Eq. (9) and the dashed-dotted line shows the dependence given by Eq. (10).

given by Eqs. (24a) and (24b). The results are presented for different values of the nonlinearity parameter β. One can see that the proposed model potential is in excellent agreement with the exact solution up to $\beta \sim 100$. Other comparisons (not shown in Fig. 5) also confirmed that the proposed model potential can be reliably used to approximate the potential distribution with good accuracy for typical experimental conditions.

It should be noted, in addition, that using the potential (16), one can also obtain a simple approximation to the exact potential distribution at small distances from the particle ($r \sim 1 - 2\lambda_{Di}$). Namely, evaluating the inverse screening length given by Eq. (20) at $y_s = k_0^{-1}$, one obtain

$$k_s = k_0[\hat{k}_* + (1 - \hat{k}_*)\ln(\cosh(\hat{c}_*))/\hat{c}_*],$$

where $k_s = k(y_s)$ and $\hat{k}_* = k_*/k_0$, $\hat{c}_* = c_*/k_0$. Note that the ratio k_s/k_0 depends only on the parameter β, that follows from Eqs. (24a) and (24b). It can be shown that this dependence is rather well approximated by the following function:

$$k_s/k_0 = (1 + 0.48\sqrt{\beta})^{-1/2}.$$

The corresponding screening length is then given by

$$\lambda_s/\lambda_D = \sqrt{1 + 0.48\sqrt{\beta}}. \tag{25}$$

One can expect that the DH potential with the effective screening length (25) can provide a good approximation to the exact potential distribution at small distances from the particle ($r \lesssim \lambda_{Di}$).

It can be seen that Eq. (25) differs from the analogous dependencies given by Eqs. (9) and (10). We show the comparison between these dependencies in Fig. 6. Note that for clarity we used λ_D instead of λ_{Di} in Eqs. (9) and (10) to make the comparison with Eq. (25). One can see from Fig. 6 that the dependence (25) is rather close to the dependence (9) at small vales of β. It is obvious, since for $\beta \ll 1$ the dependence (25) can be approximated by the linearized expression $\lambda_s/\lambda_D \approx 1 + 0.24\sqrt{\beta}$, which is indeed very similar to the dependence (9). However, at high values of β, the dependence (25) scales as $\beta^{1/4}$ rather than $\beta^{1/2}$. One can also see that the dependence (10) differs from the dependencies (9) and (25) both in the linear and nonlinear regimes. It can be explained by the fact that the function (10) was derived using the results of Ref. 18 obtained on the basis of a simplified model (see comment after Eq. (10) in Sec. II).

It is interesting to note that the scaling of the dependence (25) in the nonlinear regime can be qualitatively explained as follows. When the ion-particle coupling is sufficiently strong, the charge density near the particle is approximately proportional to $\sqrt{\varphi_i}$. For example, using the function (13), one can write the following model equation for the potential near the particle

$$\Delta\varphi_i = 2\sqrt{\varphi_i/\pi}, \tag{26a}$$

where r is normalized to λ_{Di}. Introducing the screening factor φ_s as $\varphi_e = \alpha_e\,\varphi_s/x$, we obtain from Eq. (26a)

$$\frac{\partial^2\varphi_s}{\partial r^2} = 2\,(\pi\beta)^{-1/2}\sqrt{\varphi_s r}. \tag{26b}$$

If we consider Eq. (26b) at $r \sim 1$ (i.e., in the region near λ_{Di}) and neglect the factor $\sqrt{r}$, we obtain the following solution:[22]

$$\varphi_s = (1 - \tilde{k}_s(r-1))^4, \tag{26c}$$

where $\tilde{k}_s = (36\,\pi\beta)^{-1/4}$. Here, the parameter $\tilde{k}_s$ can be interpreted as an inverse screening length. Therefore, in this case, the screening length scales as $\beta^{1/4}$. This would be a possible qualitative explanation of the dependence (25) at high values of β.

The comparison between the exact solution and the DH potential with the effective screening lengths given by Eqs. (9), (10), and (25) is presented in Fig. 7 for two different values of the nonlinearity parameter. For comparison,

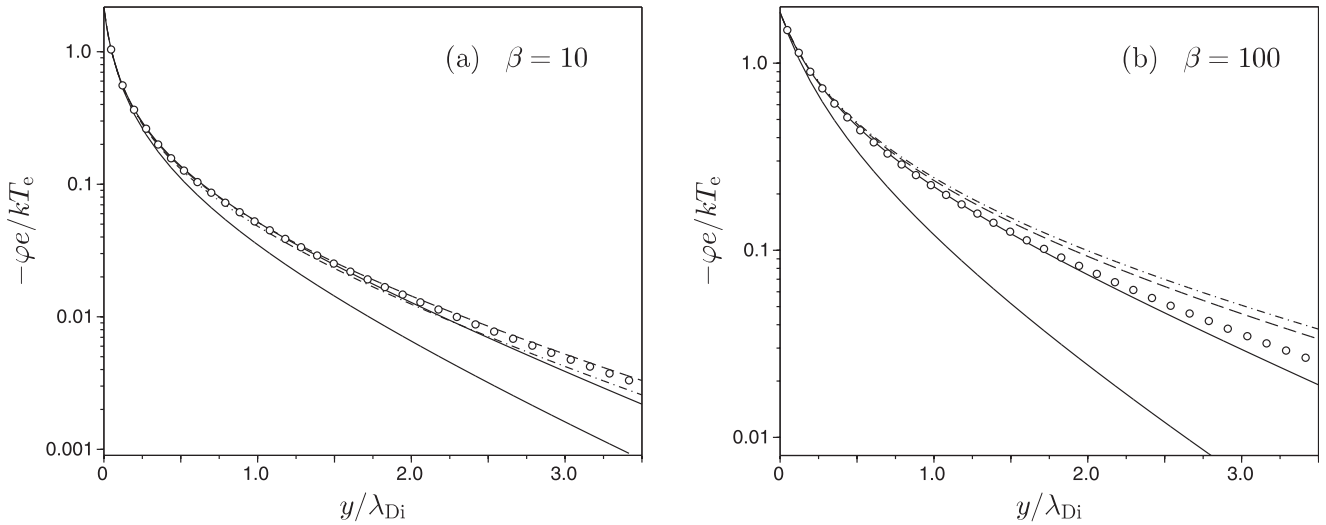

FIG. 7. The electric potential distribution near the particle for two different values of the nonlinearity parameter: $\beta = 10$ (a) and $\beta = 100$ (b). The corresponding values of τ_e and a are the same as in Fig. 1. The solid line shows the numerical solution of the nonlinear Poisson equation (1), the circles show the DH potential with the screening length given by Eq. (25), the dashed line shows the DH potential with the screening length given by Eq. (9), the dashed-dotted line shows the DH potential with the screening length given by Eq. (10) and the dotted line shows the DH potential with the linearized Debye length λ_D.

we also show the DH potential with the linearized Debye length. One can see from Fig. 7 that the DH potential with fixed effective screening length does provide a good approximation to the exact solution at relatively small distances from the particle ($r \sim 1 - 2\lambda_{Di}$). For moderate values of β (Fig. 7(a)), the approximations obtained using Eqs. (9), (10), and (25) are all close to the exact potential distribution. However, at high values of β (Fig. 7(b)), the DH potential with the screening length (25) provides slightly better approximation to the exact solution than those obtained using Eqs. (9) and (10). One can conclude, therefore, that Eq. (25) gives a more accurate expression for the effective screening length than the expressions (9) and (10).

Finally, let us discuss the conditions of applicability of the model potential described in Secs. III A and III B. Generally speaking, these conditions are given by $a \ll \lambda_{Di}$ and $T_e \gg T_i$. The first condition allows one to neglect the influence of the far-field asymptote (6b) on the potential distribution in the region of interest ($r \lesssim 10\lambda_{Di}$). In this case, the model potential can be written in the form (11). Moreover, the condition $a \ll \lambda_{Di}$ allows one to use the OML flux balance equation for calculating the particle surface potential. Our results showed that a reasonable limitation on the particle size is $a \lesssim 0.2\lambda_{Di}$. Note that this condition is satisfied in most experiments with complex plasmas. The condition $T_e \gg T_i$ is related to the applicability of the expressions (24a) and (24b) for the parameters of the model. Our computations showed that the universal dependence on β described by Eqs. (24a) and (24b) is valid for $T_e/T_i \gtrsim 10$. This condition is also satisfied in most experiments, since typical values of the electron-to-ion temperature ratio in gas discharges are $T_e/T_i \sim 100$. It should be noted that for smaller values of T_e/T_i the parameters of the model potential can still be obtained using the procedure described in Sec. III B. Thus, the proposed model potential can also be used, for example, to approximate the potential distribution around the particles in thermal plasmas.

IV. CONCLUSIONS

To summarize, we propose a new approximate expression for the electric potential around an absorbing particle in isotropic collisionless plasma. The model potential is given by the sum of the Debye-Hückel potential with an effective screening length and the far-field asymptote obtained from the solution of the linearized Poisson equation. In contrast to the existing models,[18,19] the effective screening length is not fixed but depends on the distance from the particle. The expression for the effective screening length contains two adjustable parameters which are obtained using the procedure based on charge balance considerations. For typical conditions used in the experiments with complex plasmas, the parameters of the model are shown to depend only on the nonlinearity parameter β. Simple approximations to the corresponding dependencies are suggested.

The proposed model potential is compared with the exact potential distribution obtained by solving the nonlinear Poisson equation with charge density derived from the solution of the Vlasov equation. The comparison shows excellent agreement between the model potential and the exact solution in the entire range of distances from the particle for the nonlinearity parameter varied in the range $\beta \lesssim 100$. The conditions of applicability of the model are estimated as $a \lesssim 0.2\lambda_{Di}$ and $T_e/T_i \gtrsim 10$. Therefore, the proposed model potential can be reliably used to approximate the potential distribution with good accuracy for typical experimental conditions.

In addition, we show that the Debye-Hückel potential with the characteristic screening length estimated using the proposed model provides a good approximation to the exact potential distribution at relatively small distances from the particle ($r \sim \lambda_{Di}$). In this case, the effective screening length also depends only on the parameter β. The corresponding dependence is shown to be more accurate than the analogous dependencies proposed previously.[19,20]

The results obtained in this work can be useful for understanding various experimental observations in complex

plasmas. In particular, they can be important for understanding the properties of three dimensional particle structures studied in microgravity experiments.

ACKNOWLEDGMENTS

At a late stage of this work, S.A.K. has been supported by the A*MIDEX grant (Nr. ANR-11-IDEX-0001-02) funded by the French Government "Investissements d'Avenir" program.

[1]V. N. Tsytovich, G. E. Morfill, and H. Thomas, Plasma Phys. Rep. **28**, 623 (2002).
[2]G. E. Morfill, V. N. Tsytovich, and H. Thomas, Plasma Phys. Rep. **29**, 1 (2003).
[3]V. E. Fortov, A. V. Ivlev, S. A. Khrapak, A. G. Khrapak, and G. E. Morfill, Phys. Rep. **421**, 1 (2005).
[4]V. E. Fortov and G. E. Morfill, *Complex and Dusty Plasmas: From Laboratory to Space* (CRC Press, 2009).
[5]H. Thomas, G. E. Morfill, and V. N. Tsytovich, Plasma Phys. Rep. **29**, 895 (2003).
[6]G. E. Morfill and A. V. Ivlev, Rev. Mod. Phys. **81**, 1353 (2009).
[7]M. Bonitz, C. Henning, and D. Block, Rep. Prog. Phys. **73**, 066501 (2010).
[8]G. E. Morfill, H. M. Thomas, U. Konopka, H. Rothermel, M. Zuzic, A. Ivlev, and J. Goree, Phys. Rev. Lett. **83**, 1598 (1999).
[9]H. M. Thomas, G. E. Morfill, V. E. Fortov, A. V. Ivlev, V. I. Molotkov, A. M. Lipaev, T. Hagl, H. Rothermel, S. A. Khrapak, R. K. Suetterlin, M. Rubin-Zuzic, O. F. Petrov, V. I. Tokarev, and S. K. Krikalev, New J. Phys. **10**, 033036 (2008).
[10]M. A. Fink, M. H. Thoma, and G. E. Morfill, Microgravity Sci. Technol. **23**, 169 (2011).
[11]A. Bouchoule, *Dusty Plasmas: Physics, Chemistry, and Technological Impacts in Plasma Processing* (John Wiley & Sons Inc, 1999).
[12]D. A. Mendis, Plasma Sources Sci. Technol. **11**, A219 (2002).
[13]A. Y. Pigarov, S. I. Krasheninnikov, T. K. Soboleva, and T. D. Rognlien, Phys. Plasmas **12**, 122508 (2005).
[14]U. de Angelis, Phys. Plasmas **13**, 012514 (2006).
[15]T. Bystrenko and A. Zagorodny, Phys. Lett. A **299**, 383 (2002).
[16]X.-Z. Tang and G. L. Delzanno, Phys. Plasmas **21**, 123708 (2014).
[17]S. Khrapak, A. Ivlev, G. Morfill, and H. Thomas, Phys. Rev. E **66**, 046414 (2002).
[18]J. E. Dougherty, R. K. Porteous, M. D. Kilgore, and D. B. Graves, J. Appl. Phys. **72**, 3934 (1992).
[19]S. Ratynskaia, U. de Angelis, S. Khrapak, B. Klumov, and G. Morfill, Phys. Plasmas **13**, 104508 (2006).
[20]S. Khrapak and G. Morfill, Contrib. Plasma Phys. **49**, 148 (2009).
[21]J. E. Allen, B. M. Annaratone, and U. de Angelis, J. Plasma Phys. **63**, 299 (2000).
[22]V. Tsytovich, N. Gusein-Zade, and G. Morfill, IEEE Trans. Plasma Sci. **32**, 637 (2004).
[23]I. H. Hutchinson, Plasma Phys. Controlled Fusion **45**, 1477 (2003).